Impact of non-stoichiometry on ion migration and photovoltaic performance of Formamidinium-based Perovskite Solar Cells

–Electronic Supplementary Information

Stijn Lammar[1#], *Renán Escalante*[2#], *Antonio J. Riquelme*[2], *Sandra Jenatsch*[3], *Beat Ruhstaller*[3], Prof. *Gerko Oskam*[2,4], *Prof. Tom Aernouts*[1*], and *Prof. Juan A. Anta*[2,*]

Experimental details of device fabrication with mixed perovskite.

The following procedures were carried out:

Solution preparation

1. PTAA was dissolved in Toluene at a concentration of 2 mg/ml.
2. The 1.245M stoichiometric perovskite solution was prepared by mixing 1.245 mmol PbI_2, 0.1245 mmol CsI, 0.9524 mmol FAI and 0.1681 mmol FABr in 1 ml of mixed solvents composed of 0.9 ml DMF and 0.1 ml NMP. The solution is stirred at room temperature for 2 days before use. The excess of FAI was added with respect to the PbI_2 content of the stoichiometric solution: 1.0%, 1.5%, 2.0% and 2.5% correspond with an additional 0.01245 mmol, 0.018675 mmol, 0.0249 mmol and 0.031125 mmol FAI, respectively.

Device fabrication

The ITO coated glass substrates, with an area of 3x3 cm^2, were subsequently cleaned using detergent, deionized water, acetone and isopropanol by sonicating for 5-10 min in each solvent. After drying with a nitrogen pressure gun, the substrates were transferred to a nitrogen filled glovebox.
First, a PTAA (2 mg/ml in Toluene) was dynamically spin coated at 5500 rpm for 35s, after which the substrate was annealed for 10 min at 100 C. Afterwards, the samples were cooled before proceeding with the perovskite layer. Next, the perovskite solution was dynamically spin coated by a continuous two-step program: 2000 rpm for 10 s and then 5000 rpm for 30 s. During the second step, the perovskite film was quenched with nitrogen for 15s, starting at 25 s prior to to end of the spin coating program. Afterwards, the films were annealed at 130 C for 20 min. Next, 40 nm C60 and 5 nm BCP were thermally evaporated in a high

vacuum chamber (~ 10^{-7} Torr) at a deposition rate of 0.5 A/s for both materials. Finally, a 100 nm thick copper (Cu) layer was thermally evaporated at a rate of 2 A/s to finish the PSC.

Table S1. Details of chemicals used.

Materials	Suplier
Indium tin oxide (ITO) coated glass substrates	Colorado Concept Coatings LLC
Lead iodide (PbI_2)	Tokyo Chemical Industry (TCI)
Formamidinium iodide (FAI)	Greatcellsolar Materials
Formamidinium bromide (FABr)	Greatcellsolar Materials
Cesium iodide (CsI)	Tokyo Chemical Industry (TCI)
Fullerene C_{60}	Nano-c
Bathocuproine (BCP)	Luminescence Technology Corp. (Lumtec)
Poly[bis(4- phenyl) (2,4,6- trimethylphenyl) amine] (PTAA)	Flexink
Copper (Cu)	Angstrom Engineering
Anhydrous N, N-Dimethylformamide anhydrous, 99.8% (DMF)	Sigma-Aldrich
Anhydrous 1-methyl-2-pyrrolidone (NMP)	Sigma-Aldrich
Anhydrous isopropanol (IPA)	Sigma-Aldrich
Anhydrous Toluene	Sigma-Aldrich

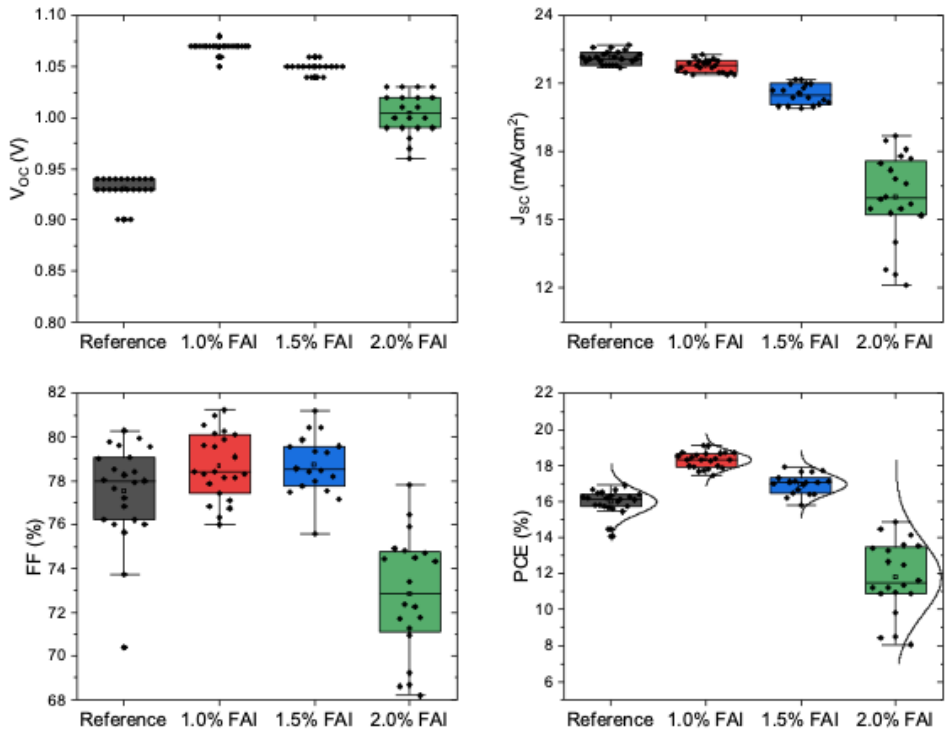

Figure S1. Photovoltaic parameters and statistics of non-stoichiometric devices.

Table S2. Hysteresis index and photovoltaic parameters in scan-rate dependent measurements of the studied PSC. The JV curves were taken from faster to slower scan rates. The conditional colour for the columns of maximum power, V_{OC}, J_{SC} and FF are shown in green for the better and red for the worse.

			Reverse				Forward			
		DoH	MaxPot	FF	Voc	Jsc	MaxPot	FF	Voc	Jsc
		%	mW/cm²		V	mA/cm²	mW/cm²		V	mA/cm²
REF-UPO-10	ScanRate 0.001	7.97	2.85	0.79	0.958	3.8	2.68	0.81	0.874	3.8
	ScanRate 0.01	2.41	2.85	0.79	0.957	3.8	2.83	0.81	0.926	3.8
	ScanRate 0.05	2.13	2.84	0.79	0.960	3.8	2.82	0.80	0.935	3.8
	ScanRate 0.1	2.29	2.85	0.79	0.960	3.8	2.84	0.81	0.938	3.7
	ScanRate 0.2	3.49	2.87	0.79	0.962	3.8	2.81	0.80	0.940	3.7
	ScanRate 0.4	5.58	2.92	0.80	0.965	3.8	2.75	0.78	0.940	3.7
	ScanRate 0.6	7.11	2.95	0.80	0.965	3.8	2.70	0.76	0.938	3.8
	ScanRate 0.8	8.28	2.97	0.80	0.964	3.9	2.66	0.75	0.938	3.8
	ScanRate 1	9.28	2.98	0.80	0.965	3.9	2.62	0.73	0.936	3.8
1% FAI - UPO-12	ScanRate 0.001	-0.03	3.40	0.78	0.981	4.4	3.47	0.81	0.970	4.4
	ScanRate 0.01	-1.42	3.42	0.78	0.987	4.4	3.56	0.82	0.982	4.4
	ScanRate 0.05	-0.80	3.43	0.78	0.989	4.4	3.52	0.81	0.987	4.4
	ScanRate 0.1	0.12	3.45	0.78	0.991	4.4	3.50	0.80	0.984	4.4
	ScanRate 0.2	1.35	3.51	0.79	0.994	4.5	3.47	0.79	0.984	4.4
	ScanRate 0.4	2.78	3.55	0.79	0.997	4.5	3.43	0.78	0.981	4.5
	ScanRate 0.6	3.43	3.54	0.78	0.999	4.6	3.44	0.78	0.977	4.5
	ScanRate 0.8	3.61	3.52	0.77	0.994	4.6	3.47	0.78	0.967	4.6
	ScanRate 1	4.78	3.35	0.76	0.947	4.7	3.33	0.79	0.906	4.6
1.5%FAI -UPO-14	ScanRate 0.001	-2.88	3.72	0.76	0.992	4.9	3.98	0.81	1.004	4.9
	ScanRate 0.01	-1.91	3.80	0.79	0.992	4.9	3.98	0.82	0.999	4.9
	ScanRate 0.05	-0.47	3.84	0.79	0.994	4.9	3.91	0.81	0.994	4.9
	ScanRate 0.1	0.33	3.88	0.79	0.996	4.9	3.88	0.80	0.994	4.9
	ScanRate 0.2	1.49	3.94	0.79	1.004	4.9	3.85	0.79	0.994	4.9
	ScanRate 0.4	2.62	4.02	0.80	1.011	5.0	3.83	0.78	0.992	5.0
	ScanRate 0.6	2.56	4.06	0.79	1.016	5.0	3.86	0.78	0.992	5.0
	ScanRate 0.8	4.35	4.05	0.78	1.021	5.1	3.91	0.78	0.994	5.1
	ScanRate 1	2.76	4.00	0.76	1.026	5.1	4.00	0.79	0.994	5.1
2.0%FAI -UPO-16	ScanRate 0.001	-14.38	1.98	0.60	0.945	3.5	2.81	0.81	0.977	3.6
	ScanRate 0.01	-9.15	2.07	0.65	0.950	3.3	2.56	0.78	0.963	3.4
	ScanRate 0.05	-3.01	2.17	0.69	0.953	3.3	2.31	0.73	0.958	3.3
	ScanRate 0.1	-0.93	2.24	0.71	0.955	3.3	2.26	0.71	0.955	3.3
	ScanRate 0.2	1.18	2.35	0.73	0.958	3.4	2.24	0.69	0.955	3.4
	ScanRate 0.4	3.23	2.50	0.75	0.960	3.4	2.26	0.69	0.955	3.4
	ScanRate 0.6	3.93	2.63	0.77	0.967	3.5	2.36	0.70	0.957	3.5
	ScanRate 0.8	3.37	2.73	0.77	0.974	3.7	2.55	0.73	0.963	3.6
	ScanRate 1	1.95	2.91	0.76	0.999	3.8	2.90	0.78	0.977	3.8
2.5%FAI -UPO-18	ScanRate 0.001	-35.13	1.16	0.41	0.891	3.2	2.52	0.79	0.957	3.3
	ScanRate 0.01	-20.12	1.18	0.49	0.916	2.6	1.67	0.65	0.935	2.7
	ScanRate 0.05	-8.88	1.24	0.55	0.921	2.5	1.40	0.60	0.928	2.5
	ScanRate 0.1	-5.44	1.31	0.57	0.923	2.5	1.40	0.60	0.926	2.5
	ScanRate 0.2	-2.18	1.43	0.60	0.926	2.6	1.44	0.60	0.925	2.6
	ScanRate 0.4	1.18	1.61	0.63	0.930	2.7	1.53	0.60	0.928	2.7
	ScanRate 0.6	2.62	1.83	0.66	0.936	2.9	1.69	0.62	0.933	2.9
	ScanRate 0.8	2.07	2.07	0.68	0.942	3.2	2.01	0.66	0.940	3.2
	ScanRate 1	-0.05	2.50	0.71	0.972	3.6	2.65	0.76	0.965	3.6

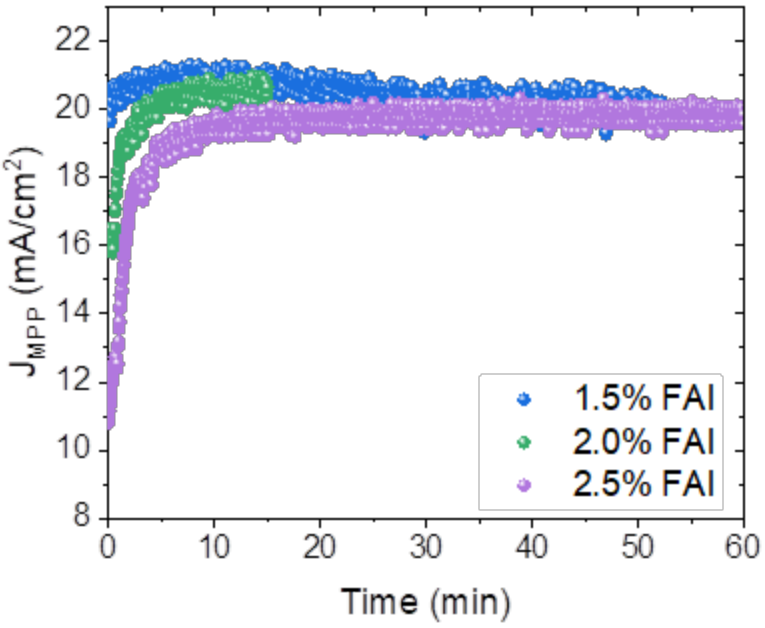

Figure S2. Photocurrent at the maximum power point under 1-sun light soaking.

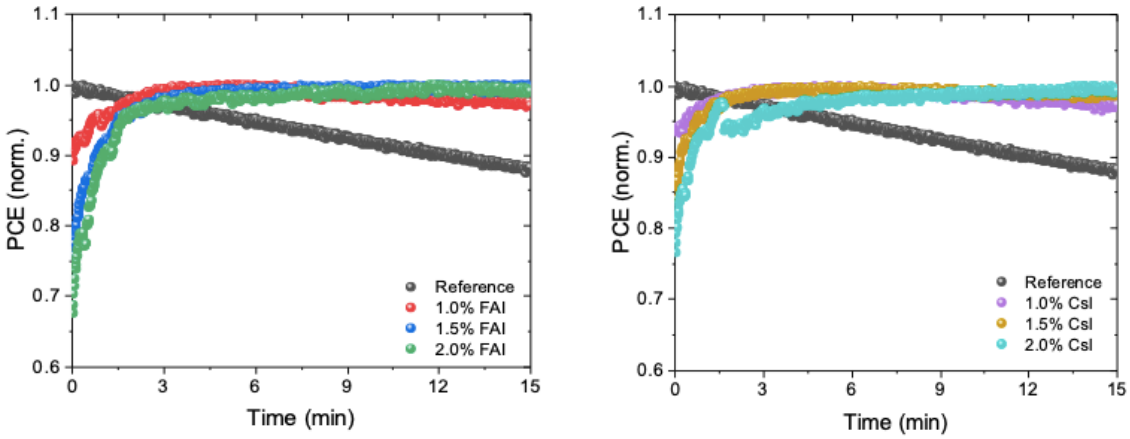

Figure S3. Photoconversion efficiency at the maximum power point under 1-sun light soaking when both FAI (left) and CsI (right) excess is modified.

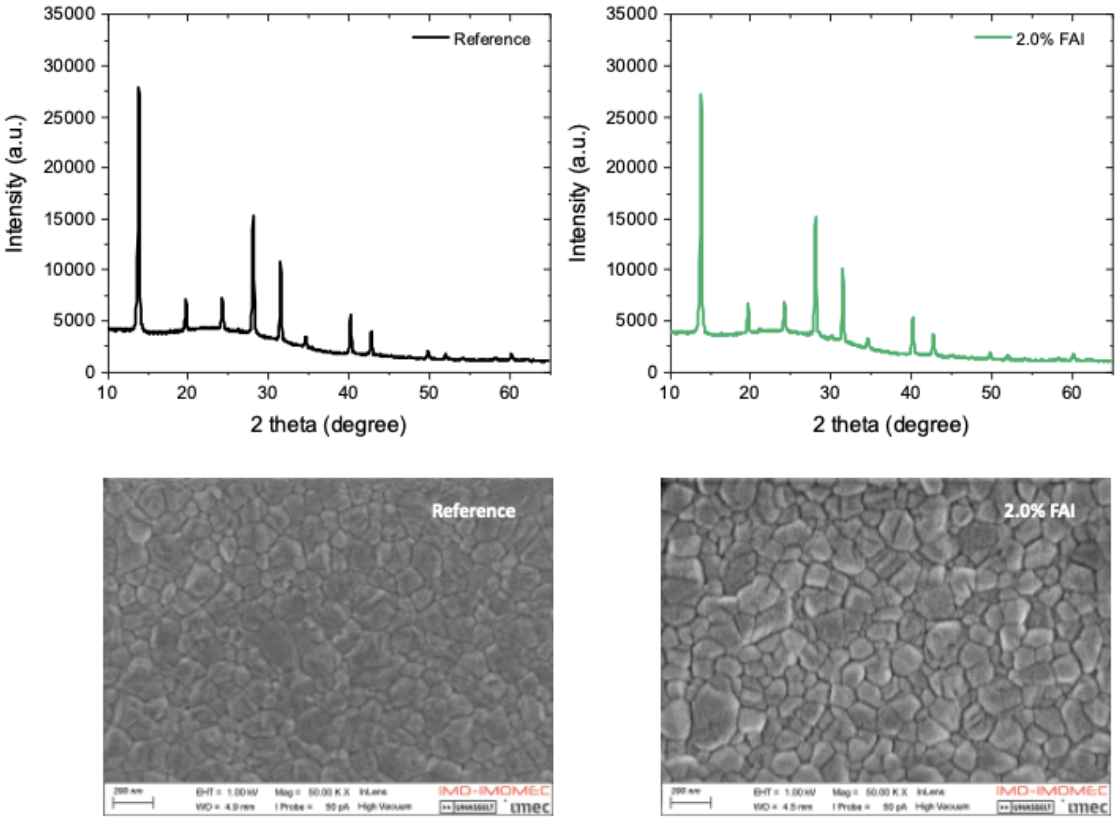

Figure S4. XRD patterns and SEM images of both reference and non-stoichiometric samples.

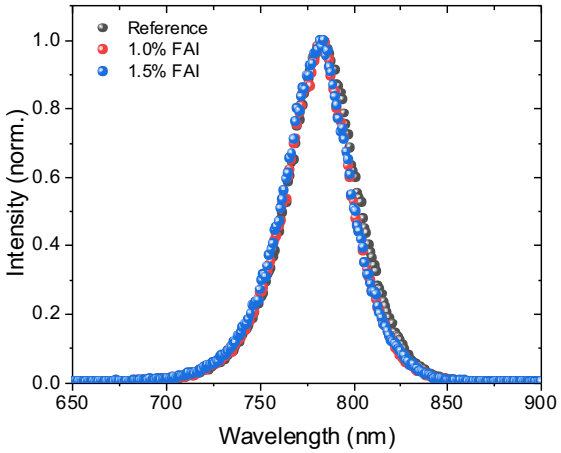

Figure S5. Photoluminiscence emission spectrum of the perovskite films

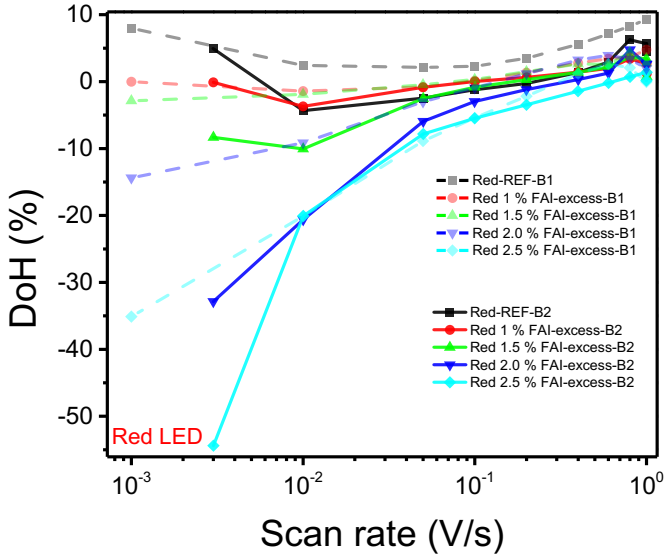

Figure S6. Hysteresis index under red light illumination as a function of the scan rate for the studied PSCs. Batch 1 (B1) was measured from faster to slower scan rates, while batch 2 (B2) was measured from slow to faster scan rates. In both measurements the DoH was obtained from a reverse scan followed by a forward one.

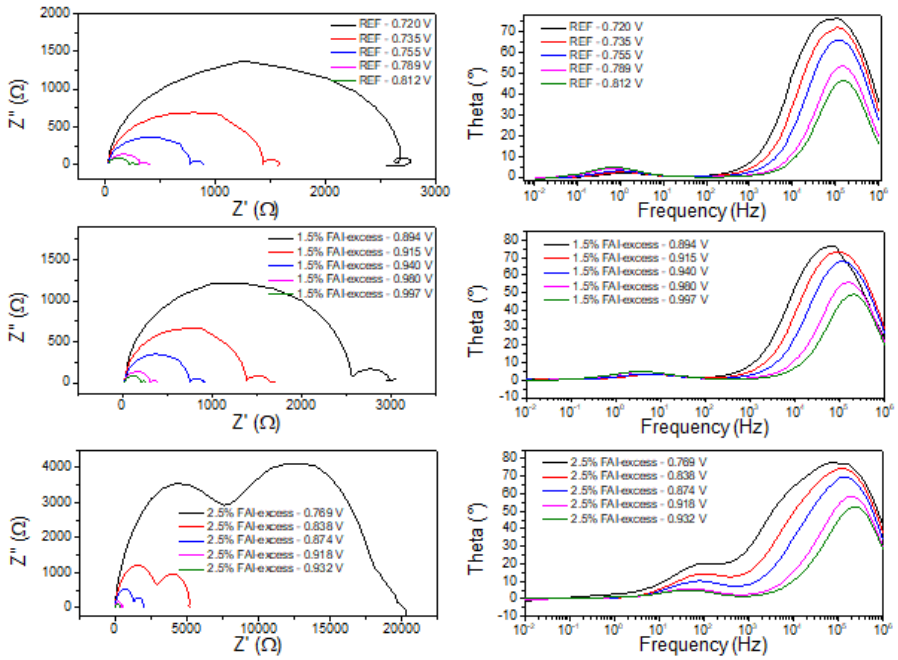

Figure S7. Nyquist plot and frequency plots of the impedance response at open circuit for the lowest and the highest FAI excess.

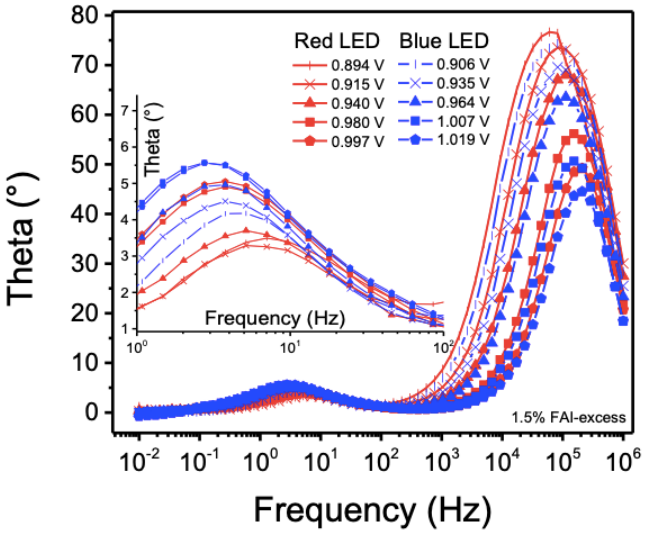

Figure S8. Frequency plot for two excitation wavelengths.

Drift-diffusion simulations.

Numerical drift-diffusion (DD) modelling was employed to simulate the coupled ion/electron dynamics and obtain theoretical IV curves and impedance spectra. We use software SETFOS 5.3 (Fluxim)[1] for this task. The absorption profile is calculated based on a transfer matrix formalism for the coherent stack using the refractive index dispersion of all the layers. It is assumed that charges are only created in the perovskite layer with a certain optical generation efficiency such that the short-circuit current density under 1 sun matches the experiment. The generation profile G(x) is hence calculated from the product of absorption profile multiplied with the generation efficiency.

The DD code solves numerically continuity equations for the stack layer: **glass/ITO/PTAA/PS/C60/BCP/Cu** where PS is the perovskite active layer. Within all semiconductor layers, the electron and hole densities, n and p respectively, are governed in time, t, and one spatial dimension, x, via the continuity equations

$$\frac{\partial n(x,t)}{\partial t} - \frac{1}{q}\frac{\partial j_n}{\partial x} = G(x) - R(x), \qquad j_n = -n(x,t)q\mu_n \frac{\partial \phi}{\partial x} + \mu_n k_B T \frac{\partial n(x,t)}{\partial x} \tag{S1}$$

$$\frac{\partial p(x,t)}{\partial t} + \frac{1}{q}\frac{\partial j_p}{\partial x} = G(x) - R(x), \qquad j_n = -p(x,t)q\mu_p \frac{\partial \phi}{\partial x} - \mu_p k_B T \frac{\partial p(x,t)}{\partial x} \tag{S2}$$

where q is the elementary charge, $\mu_{n,p}$ the respective electronic mobilities, k_B the Boltzmann constant and T is the temperature. G is the charge generation profile which considers the measured illumination spectrum, the complex refractive indices and the thickness of each layer of the cell stack. R is the total recombination profile, which includes bimolecular, trapping-mediated recombination (Shockley-Read-Hall) and surface recombination terms.[2,3]

$$R(n,p) = \beta\left(np - n_i^2\right) + \frac{(np - n_i^2)}{\tau_n p + \tau_p n} \quad \text{(S3)}$$

where β is the bimolecular recombination coefficient and τ_n, τ_p are the electron and hole pseudolifetimes (mid band gap approximation).

The migration of the mobile anions (A) and cations (C) is modelled via

$$\frac{\partial A(x,t)}{\partial t} = \frac{1}{q}\frac{\partial j_a}{\partial x} \qquad j_n = -A(x,t)q\mu_a\frac{\partial \phi}{\partial x} + \mu_a k_B T\frac{\partial A(x,t)}{\partial x} \quad \text{(S4)}$$

$$\frac{\partial C(x,t)}{\partial t} = \frac{1}{q}\frac{\partial j_c}{\partial x}, \qquad j_n = -C(x,t)q\mu_c\frac{\partial \phi}{\partial x} - \mu_c k_B T\frac{\partial C(x,t)}{\partial x} \quad \text{(S5)}$$

where J_a , J_p are the ionic fluxes and $\mu_{a,c}$ the respective ionic mobilities. The motion of ions is restricted to the perovskite layer. Equations (S1-S5) couple to Poisson's equation for the electric potential

$$\frac{\partial^2 \phi}{\partial x^2} = \frac{q}{\epsilon_p}(C - A + n - p). \quad (4)$$

Here, ϵ_p(x) is the permittivity of the perovskite layer.

More details on the numerical solution of the optical and electronic equations in the full stack can be found in Ref. [3]

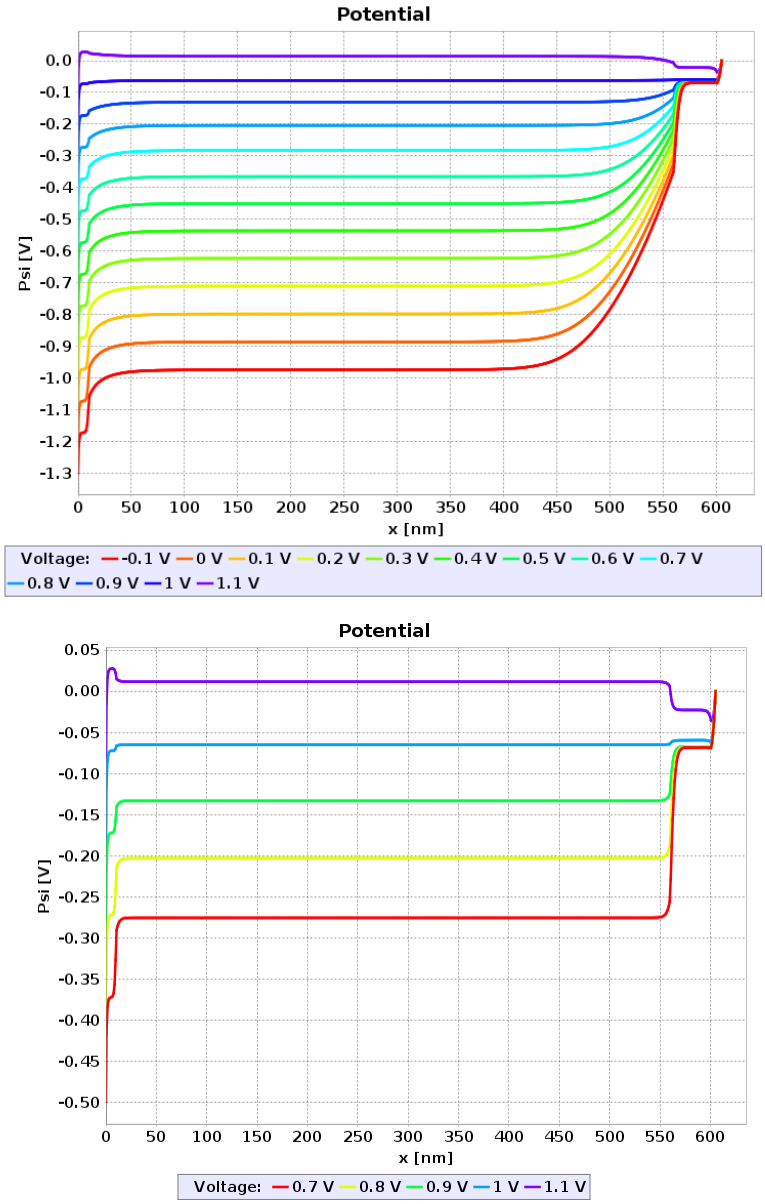

Figure S9. SETFOS snapshots showing stationary electric potential profiles for various values of the applied voltage and two values of the ionic density (10^{23} m^{-3}, top, 5 10^{24} m^{-3} bottom)

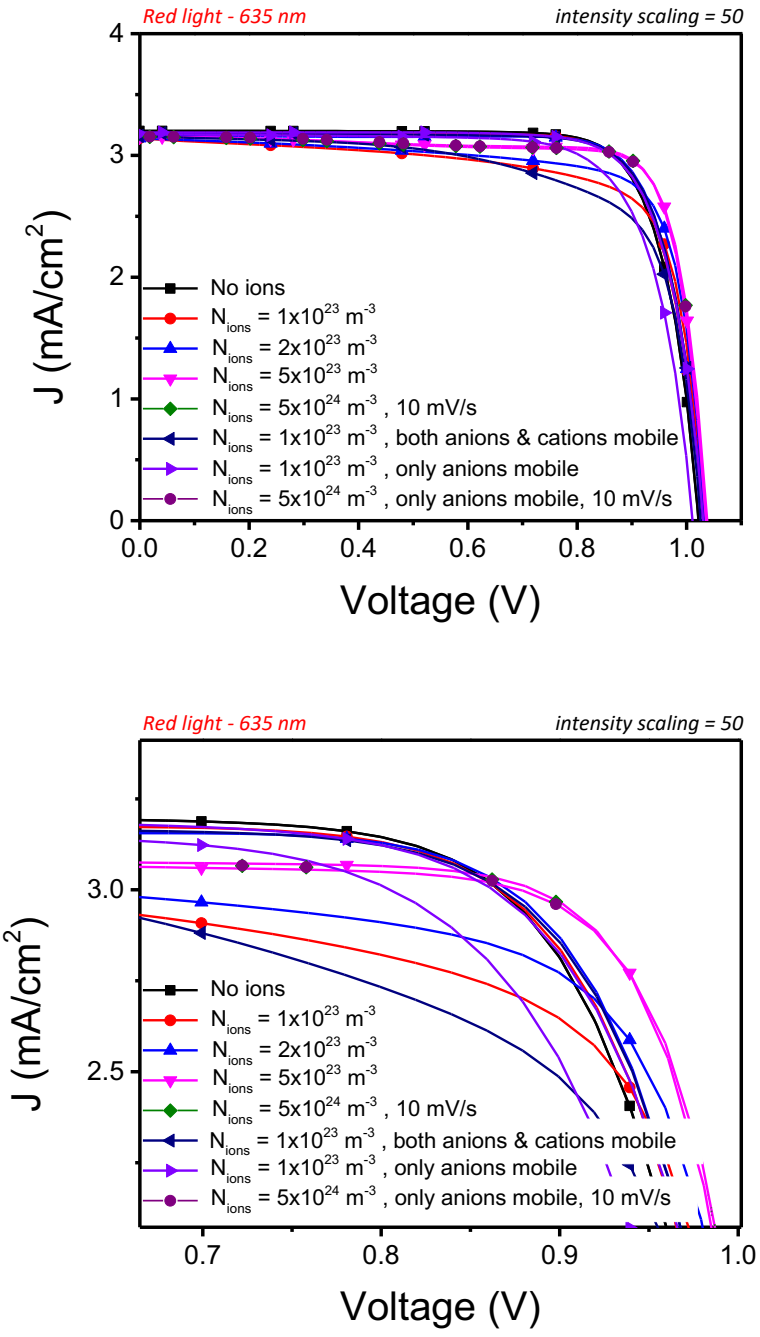

Figure S10. Transient current-voltage curves for several choices of the ionic numerical parameters and the scan rate. A blow-up of the intermediate voltage zone is shown below.

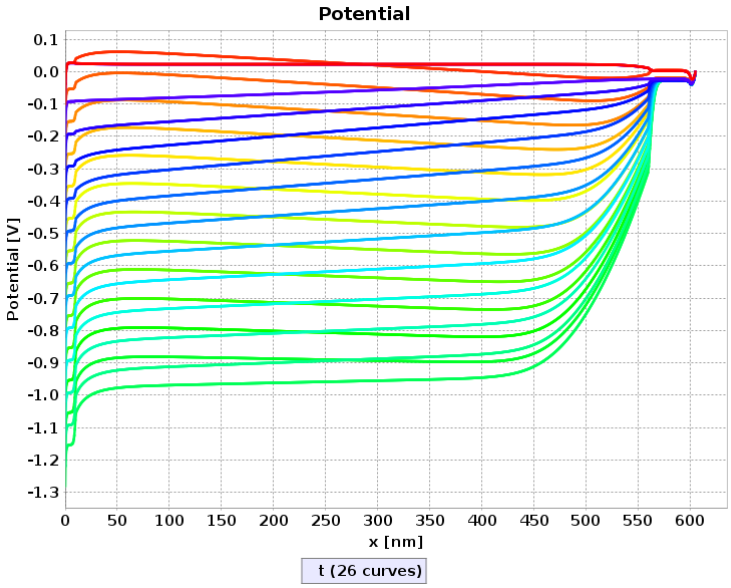

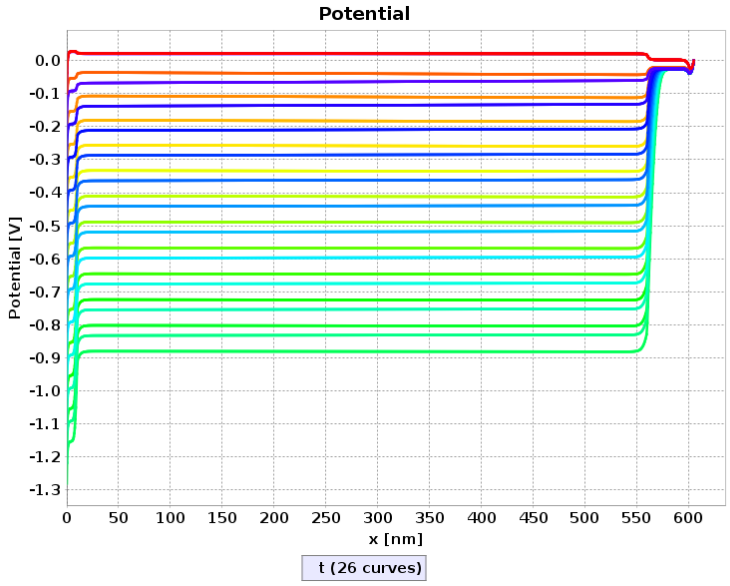

Figure S11. SETFOS snapshots showing transient electric potential profiles in the 1.1 – 0.1 V interval and 100 mV/s of scan rate. Results shown correspond to two values of the ionic density (10^{23} m^{-3} , top, 5 10^{24} m^{-3} bottom)

References

1 Fluxim AG, .

2 J. Nelson, *The Physics of Solar Cells*, Imperial College Press, 1st edn., 2003.

3 M. T. Neukom, A. Schiller, S. Züfle, E. Knapp, J. Ávila, D. Pérez-del-Rey, C. Dreessen, K. P. S. Zanoni, M. Sessolo, H. J. Bolink and B. Ruhstaller, *ACS Appl. Mater. Interfaces*, 2019, 11, 23320–23328.